Published in final edited form as:
Oncogene. 2009 January 29; 28(4): 509–517. doi:10.1038/onc.2008.407.

PTEN deficiency accelerates tumour progression in a mouse model of thyroid cancer

CJ Guigon[1], **L Zhao**[1], **MC Willingham**[2], and **S-Y Cheng**[1]

[1]Laboratory of Molecular Biology, Center for Cancer Research, National Cancer Institute, Bethesda, MD, USA

[2]Department of Pathology, Wake Forest University, Winston-Salem, NC, USA

Abstract

Inactivation and silencing of *PTEN* have been observed in multiple cancers, including follicular thyroid carcinoma. PTEN (phosphatase and tensin homologue deleted from chromosome 10) functions as a tumour suppressor by opposing the phosphatidylinositol 3-kinase (PI3K)/protein kinase B (AKT) signalling pathway. Despite correlative data, how deregulated PTEN signalling leads to thyroid carcinogenesis is not known. Mice harbouring a dominant-negative mutant thyroid hormone receptor β (*TRβ*$^{PV/PV}$ mice) spontaneously develop follicular thyroid carcinoma and distant metastases similar to human cancer. To elucidate the role of PTEN in thyroid carcinogenesis, we generated *TRβ*$^{PV/PV}$ mice haploinsufficient for *Pten* (*TRβ*$^{PV/PV}$*Pten*$^{+/-}$ mouse). PTEN deficiency accelerated the progression of thyroid tumour and increased the occurrence of metastasis spread to the lung in *TRβ*$^{PV/PV}$*Pten*$^{+/-}$ mice, thereby significantly reducing their survival as compared with *TRβ*$^{PV/PV}$*Pten*$^{+/+}$ mice. AKT activation was further increased by two-fold in *TRβ*$^{PV/PV}$*Pten*$^{+/-}$ mice thyroids, leading to increased activity of the downstream mammalian target of rapamycin (mTOR)–p70S6K signalling and decreased activity of the forkhead family member FOXO3a. Consistently, cyclin D1 expression was increased. Apoptosis was decreased as indicated by increased expression of nuclear factor-κB (NF-κB) and decreased caspase-3 activity in the thyroids of *TRβ*$^{PV/PV}$*Pten*$^{+/-}$ mice. Our results indicate that PTEN deficiency resulted in increased cell proliferation and survival in the thyroids of *TRβ*$^{PV/PV}$*Pten*$^{+/-}$ mice. Altogether, our study provides direct evidence to indicate that *in vivo*, PTEN is a critical regulator in the follicular thyroid cancer progression and invasiveness.

Keywords

thyroid cancer; Pten; carcinogenesis; mouse model; mutations

Introduction

Thyroid cancer, the most common form of endocrine malignancy, has the fastest growing incidence of all cancers in the United States, especially among women. Thyroid cancers in humans consist of an array of different histological and biological types, but the majority of clinically important human thyroid cancers are papillary and follicular carcinomas (Schlumberger *et al.*, 1998; Sherman *et al.*, 1998). The occurrence of follicular thyroid carcinoma is one of the major criteria used to define patients with Cowden syndrome (CS).

Correspondence: Dr S-Y Cheng, Gene regulation section, Laboratory of Molecular Biology, National Cancer Institute, 37 Convent Dr, Room 5128, Bethesda MD 20892-4264, USA. chengs@mail.nih.gov.

CS is a genetically inherited disorder also characterized by an increased rate of cutaneous benign hamartomatous tumours and neoplasia in the endometrium and the mammary gland (Uppal *et al.*, 2007). Over 80% of kindred with CS have inactivating mutations of the tumour suppressor gene, *PTEN* (phosphatase and tensin homologue deleted from chromosome 10) (Liaw *et al.*, 1997; Marsh *et al.*, 1997). Many studies using either primary tumour tissues or established tumour cell lines revealed high frequencies of *PTEN* somatic mutation or deletion in various human tumours, including breast, prostate and thyroid tumours (Li *et al.*, 1997; Liaw *et al.*, 1997; Nelen *et al.*, 1997; Steck *et al.*, 1997), making *Pten* the second most frequently mutated human tumour suppressor gene next to *TP53*. Analysis of *Pten* deficiency in mice ($Pten^{+/-}$ mice) has shown the tumour suppressor role of PTEN, in that $Pten^{+/-}$ heterozygous mice develop neoplasias in multiple organs. *Pten* also plays a major role during embryonic development, as $Pten^{-/-}$ homozygous mice die *in utero* (Di Cristofano *et al.*, 1998; Suzuki *et al.*, 1998; Podsypanina *et al.*, 1999).

Pten encodes a lipid phosphatase that negatively regulates PI3K/AKT signalling by dephosphorylating phosphatidylinositol 3,4,5-phosphate at the 3′-position (Shepherd *et al.*, 1997; Neri *et al.*, 2002; Wymann and Marone, 2005). A variety of biological effects have been attributed to PTEN deficiency that is relevant to its role as a tumour suppressor gene. However, despite many correlative data, it is not known how the deregulation of the PTEN signalling cascade leads to thyroid carcinoma (Eng, 2002).

The creation of a mouse model of follicular thyroid cancer ($TR\beta^{PV/PV}$ mice) has provided a valuable tool to elucidate the molecular basis underlying thyroid carcinogenesis (Kaneshige *et al.*, 2000; Ying *et al.*, 2003). The $TR\beta^{PV/PV}$ mouse was created by a targeted mutation of the thyroid hormone β receptor (*TRβPV*) (Kaneshige *et al.*, 2000). The thyroid hormone receptor β mutant (referred to as PV) was identified in a patient (PV) with resistance to thyroid hormone (RTH) (Parrilla *et al.*, 1991). RTH is caused by mutations of the *TR*β gene and manifests symptoms as a result of decreased sensitivity to the thyroid hormone (T3) in target tissues (Yen, 2003). PV has a C insertion at codon 448 that produces a frame shift in the C-terminal 14 amino acids of TRβ1 (Parrilla *et al.*, 1991). PV has completely lost T3 binding and exhibits a potent dominant-negative activity (Meier *et al.*, 1992). As $TR\beta^{PV/PV}$ mice age, they spontaneously develop follicular thyroid carcinoma similar to human thyroid cancer with a pathological progression from hyperplasia to vascular invasion, capsular invasion, anaplasia and eventually metastasis (Kaneshige *et al.*, 2000; Suzuki *et al.*, 2002).

To understand the roles of PTEN in thyroid carcinogenesis, we adopted the loss-of-function approach by crossing $TR\beta^{PV/PV}$ mice with $Pten^{+/-}$ mice to generate $TR\beta^{PV/PV}$ mice deficient in one allele of the *Pten* gene ($TR\beta^{PV/PV}Pten^{+/-}$ mice) and evaluated the effect of PTEN deficiency on the spontaneous development of thyroid carcinogenesis. Mice lacking both alleles of the *Pten* gene are embryonic lethal and could not be studied. Here, we show that PTEN deficiency markedly increased cell proliferation and survival to promote thyroid tumour growth in $TR\beta^{PV/PV}$ mice. Strikingly, follicular thyroid cancer as well as distant metastases to the lung occurred much earlier and at a higher frequency in $TR\beta^{PV/PV}Pten^{+/-}$ mice than in $TR\beta^{PV/PV}$ mice. Our findings indicate that PTEN deficiency results in constitutive activation of the PI3K/AKT pathway to play a critical role in thyroid cancer progression and aggressiveness.

Results

PTEN deficiency promotes thyroid carcinogenesis in $TR\beta^{PV/PV}$ mice

To determine whether the loss of one *Pten* tumour suppressor gene could promote thyroid carcinogenesis, we generated $TR\beta^{PV/PV}Pten^{+/-}$ mice and compared their survival rates with those from $TR\beta^{PV/PV}Pten^{+/+}$, $TR\beta^{+/+}Pten^{+/-}$ and $TR\beta^{+/+}Pten^{+/+}$ wild-type mice. Mice were

monitored until they became moribund with signs of palpable tumour, rapid weight loss, hunched posture and laboured breathing. Analysis of the survival curves over a period of 15 months (Figure 1A) indicates that $TR\beta^{PV/PV}Pten^{+/-}$ mice died at a significantly younger age (50% survival age: 5.5 months, $n = 33$) than did either $TR\beta^{PV/PV}Pten^{+/+}$ mice (50% survival age: 10.0 months, $n = 25$) ($P < 0.01$) or $TR\beta^{+/+}Pten^{+/-}$ mice (50% survival age: 14.1 months, $n = 33$) ($P < 0.01$). In moribund $TR\beta^{PV/PV}Pten^{+/-}$ and $TR\beta^{PV/PV}Pten^{+/+}$ mice, the trachea was compressed due to the dramatic enlargement of the thyroid. In contrast, moribund $TR\beta^{+/+}Pten^{+/-}$ mice displayed normal-sized thyroid but showed a massive lymph node enlargement in the neck and axilla regions, splenomegaly and thymus enlargement, as described by others (Podsypanina *et al.*, 1999). No significant gender differences in the 50% survival age of $TR\beta^{PV/PV}Pten^{+/+}$ and $TR\beta^{PV/PV}Pten^{+/-}$ mice were observed (Table 1).

The thyroid weight was determined and expressed as the ratios of thyroid to body weight (Figure 1B). The thyroid weights of $TR\beta^{+/+}Pten^{+/-}$ mice were similar to those of $TR\beta^{+/+}Pten^{+/+}$ wild-type mice at any age studied. In contrast, $TR\beta^{PV/PV}Pten^{+/+}$ and $TR\beta^{PV/PV}Pten^{+/-}$ thyroid weights were significantly higher than those of $TR\beta^{+/+}Pten^{+/+}$ wild-type and $TR\beta^{+/+}Pten^{+/-}$ mice (Figure 1B). The thyroid weight was similar between $TR\beta^{PV/PV}Pten^{+/-}$ and $TR\beta^{PV/PV}Pten^{+/+}$ mice in the age group of 2–4 months, but it was significantly higher in $TR\beta^{PV/PV}Pten^{+/-}$ than in $TR\beta^{PV/PV}Pten^{+/+}$ mice at 5–7 months as the tumourigenesis progressed.

The effect of PTEN deficiency on thyroid tumour progression and invasiveness was evaluated by histopathological analysis. Figure 1C shows representative pathohistological features of the thyroids of $TR\beta^{+/+}Pten^{+/-}$ mice (Figure 1Ca; age: 7 months) that exhibit no apparent abnormalities. In the thyroid of $TR\beta^{PV/PV}Pten^{+/+}$ mice at the age of 7 months, capsular invasion was apparent (Figure 1Cb). However, in the thyroid of $TR\beta^{PV/PV}Pten^{+/-}$ mice, advanced capsular invasion (Figure 1Cc), vascular invasion (Figure 1Cd) and anaplasia (Figure 1Ce) were frequently observed at a younger age of 5 months. Moreover, although no metastasis was detected in $TR\beta^{PV/PV}Pten^{+/+}$ mice at 5 months, lung metastases (Figure 1 Cf) were frequently observed in $TR\beta^{PV/PV}Pten^{+/-}$ mice at the same age.

The pathohistological observations are summarized in Figure 1D. From 2 to 4 months of age, all $TR\beta^{PV/PV}Pten^{+/+}$ mice and $TR\beta^{PV/PV}Pten^{+/-}$ mice displayed advanced thyroid hyperplasia (data not shown); however, the occurrence of capsular invasion in the thyroid was found in ~40% of the $TR\beta^{PV/PV}Pten^{+/-}$ mice but in none of the $TR\beta^{PV/PV}Pten^{+/+}$ mice at the same age (Figure 1Da). Vascular invasion developed in the thyroid at 5–7 months of age in both $TR\beta^{PV/PV}Pten^{+/+}$ mice and $TR\beta^{PV/PV}Pten^{+/-}$ mice; however, it was observed in ~70% of $TR\beta^{PV/PV}Pten^{+/-}$ mice versus ~10% of $TR\beta^{PV/PV}Pten^{+/+}$ mice (Figure 1Db). It can be noted that thyroid anaplasia, which did not develop before 7 months of age in $TR\beta^{PV/PV}Pten^{+/+}$ mice, occurred at a young age of 2–4 months in $TR\beta^{PV/PV}Pten^{+/-}$ mice (Figure 1Dc). Moreover, in mice older than 7 months, a high ~50% of $TR\beta^{PV/PV}Pten^{+/+}$ mice developed anaplasia as compared with 10% occurrence in $TR\beta^{PV/PV}Pten^{+/+}$ mice (Figure 1Dc).

Importantly, metastatic lesions in the lung were detected only in $TR\beta^{PV/PV}Pten^{+/+}$ mice older than 7 months, but they occurred at a much younger age of 2–4 months in $TR\beta^{PV/PV}Pten^{+/-}$ mice (Figure 1Dd). In mice older than 7 months, the occurrence of lung metastases was significantly more frequent in $TR\beta^{PV/PV}Pten^{+/-}$ mice than in $TR\beta^{PV/PV}Pten^{+/+}$ mice (~80% in $TR\beta^{PV/PV}Pten^{+/-}$ mice versus ~10% in $TR\beta^{PV/PV}Pten^{+/+}$ mice) (Figure 1Dd). These results indicate that thyroid tumours progress significantly faster in $TR\beta^{PV/PV}Pten^{+/-}$ mice than in $TR\beta^{PV/PV}Pten^{+/+}$ mice. We further analysed whether there were gender differences in the pathological progression. Table 1 shows that female $TR\beta^{PV/PV}Pten^{+/+}$ mice had a significant higher frequency in the development of vascular

invasion than male $TR\beta^{PV/PV}Pten^{+/+}$ mice. In both $TR\beta^{PV/PV}Pten^{+/-}$ and $TR\beta^{PV/PV}Pten^{+/+}$ mice, the frequency of occurrence of metastasis was significantly higher in female mice than in male mice (Table 1).

PTEN deficiency does not affect the extent of dysregulation of the pituitary–thyroid axis in $TR\beta^{PV/PV}$ mice

We reported earlier that $TR\beta^{PV/PV}$ mice exhibit dysregulation of the pituitary–thyroid axis (Kaneshige *et al.*, 2000) with elevated serum thyroid hormone and thyroid-stimulating hormone (TSH) levels. It is known that TSH is a major regulator of thyrocyte proliferation and its levels are regulated by the thyroid hormones (L-thyroxine, T4; 3,3′,5-triodo-L-thyronine, T3) through a negative feedback loop (Rivas and Santisteban, 2003). To evaluate whether TSH could contribute to the increased thyroid growth in $TR\beta^{PV/PV}Pten^{+/-}$ mice (Figure 1B), we compared serum total T4, total T3 and TSH between $TR\beta^{PV/PV}Pten^{+/+}$ and $TR\beta^{PV/PV}Pten^{+/-}$ mice (Figure 2). The serum levels of total T4 (Figure 2a), total T3 (Figure 2b) and TSH (Figure 2c) were not significantly different between $TR\beta^{PV/PV}Pten^{+/+}$ mice and $TR\beta^{PV/PV}Pten^{+/-}$ mice. These data indicate that PTEN deficiency does not affect the pituitary–thyroid axis. Thus, the increased thyroid weight in $TR\beta^{PV/PV}Pten^{+/-}$ mice due to PTEN deficiency is not mediated by TSH (Figure 1B).

PTEN deficiency further increases AKT activation in the thyroid cancers of $TR\beta^{PV/PV}$ mice

PTEN protein levels in the thyroid were assessed by western blot analysis using mice at 2–3 and 5–6 months (Figures 3a and c, respectively). Dynactin-2 was used as loading controls (Figures 3b and f). At 2–3 months, PTEN abundance was reduced by ~2- to 3-fold in $TR\beta^{+/+}Pten^{+/-}$ and $TR\beta^{PV/PV}Pten^{+/-}$ mice lacking one allele of the *Pten* gene (compare lanes 3–4 with 1–2, and lanes 8–10 with 5–7; Figure 3a), indicating PTEN deficiency. Interestingly, at 5–6 months, PTEN protein abundance was further reduced in $TR\beta^{PV/PV}Pten^{+/-}$ mice because its levels became barely detectable (lanes 8–10; Figure 3c), suggesting that focal loss of the remaining wild-type *Pten* allele might have occurred as tumourigenesis progressed. To determine whether the decreased abundance of PTEN was accompanied by the over-activation of AKT in the thyroid, we also determined the protein levels of phosphorylated (p-AKT) (Figure 3d) and total AKT (Figure 3e). The ratios of p-AKT to total AKT levels indicate that there was an ~1.8-fold increase in the ratios of p-AKT to total AKT in $TR\beta^{+/+}Pten^{+/-}$ thyroids as compared with $TR\beta^{+/+}Pten^{+/+}$ mice (compare lanes 3–4 with 1–2). The ratios of p-AKT to total AKT were increased by ~5- to 6-fold in the thyroids of $TR\beta^{PV/PV}$ mice as compared with wild-type mice (compare lanes 5–7 with 1–2). Remarkably, the ratios of p-AKT to total AKT were increased by ~10- to 12-fold in $TR\beta^{PV/PV}Pten^{+/-}$ mice as compared with those in wild-type thyroids (compare lanes 8–10 with 1–2). These findings indicate that reduced PTEN protein abundance in the thyroids of $TR\beta^{PV/PV}Pten^{+/-}$ mice resulted in a further activation of AKT.

PTEN deficiency further activates mTOR–p70S6K signalling pathways and represses FOXO3a in $TR\beta^{PV/PV}$ thyroids

That AKT was further activated by PTEN deficiency (Figure 3) prompted us to assess whether the AKT downstream effectors were affected. AKT phosphorylates and activates the protein kinase mammalian target of rapamycin (mTOR), which is a convergence node of many signalling pathways, particularly by regulating protein translation and cell growth (Guertin and Sabatini, 2007). Activated mTOR phosphorylates and activates the protein kinase p70S6K. We therefore evaluated the protein abundance of phosphorylated and total mTOR (Figures 4a and b, respectively) and p70S6K (Figures 4d and e, respectively). There were no significant differences in the ratios of phosphorylated mTOR to total mTOR protein levels between $TR\beta^{+/+}Pten^{+/-}$ and $TR\beta^{+/+}Pten^{+/+}$ wild-type thyroids (Figures 4a and b, lanes 1–4). In contrast, $TR\beta^{PV/PV}$ thyroids displayed a significant increase in the ratios of

phosphorylated to total mTOR as compared with $TR\beta^{+/+}Pten^{+/+}$ wild-type thyroids (~3-fold) (Figures 4a and b, lanes 1–2 and 5–7, respectively) (Furuya *et al.*, 2006). This ratio was further increased by ~2-fold in $TR\beta^{PV/PV}Pten^{+/-}$ thyroids as compared with $TR\beta^{PV/PV}Pten^{+/+}$ thyroids (Figures 4a and b, compare lanes 5–7 with 8–10). Although no apparent changes in the ratios of phosphorylated to total p70S6K between $TR\beta^{+/+}Pten^{+/+}$ and $TR\beta^{+/+}Pten^{+/-}$ thyroids (Figures 4d and e, compare lanes 1–2 with 3–4), the ratios of phosphorylated to total p70S6K were increased by ~2-fold in $TR\beta^{PV/PV}Pten^{+/+}$ thyroids as compared with $TR\beta^{+/+}Pten^{+/+}$ thyroids (Figures 4d and e, compare lanes 1–2 with 5–7). The ratio of phosphorylated to total p70S6K was further increased by ~2-fold in $TR\beta^{PV/PV}Pten^{+/-}$ thyroids (Figures 4d and e, compare lanes 5–7 with 8–10).

FOXO3a, a member of the forkhead family of transcription factor FOXO, is a direct target of AKT (Greer and Brunet, 2005). When unphosphorylated, FOXO3a functions as a selective transcription factor in the nucleus, inducing the transcription of pro-apoptotic factors, and repressing the transcription of the cell-cycle promoter cyclin D1 (Ramaswamy *et al.*, 2002; Greer and Brunet, 2005). Phosphorylation of FOXO3a by AKT results in the translocation of FOXO3a from the nucleus to the cytoplasm, which leads to a decreased transcription of pro-apoptotic genes and an increased transcription of cyclin D1. We therefore determined phosphorylated and total protein levels of FOXO3a, and the ratios of phosphorylated to total protein levels (Figures 4g and h). No differences in the ratios of phosphorylated to total FOXO3a levels were observed between $TR\beta^{+/+}Pten^{+/+}$ and $TR\beta^{+/+}Pten^{+/-}$ thyroids (Figures 4g and h, compare lanes 1–2 with 3–4). In contrast, there was a ~2-fold increase in the ratio of phosphorylated to total FOXO3a in $TR\beta^{PV/PV}Pten^{+/+}$ thyroids as compared with $TR\beta^{+/+}Pten^{+/+}$ wild-type thyroids (Figures 4g and h, compare lanes 1–2 with 5–7). This ratio was further increased by ~2-to 3-fold in $TR\beta^{PV/PV}Pten^{+/-}$ mice (Figures 4g and h, compare lanes 5–7 with 8–10).

PTEN deficiency increases cell proliferation and cell survival in $TR\beta^{PV/PV}$ mice to promote thyroid tumour growth

We further examined the expression levels of a key cell-cycle regulator, cyclin D1, that is positively regulated by the mTOR–p70S6K signalling and repressed by FOXO3a (Pervin *et al.*, 2001; Ramaswamy *et al.*, 2002). Similar to our findings earlier (Kato *et al.*, 2006), cyclin D1 levels were markedly higher in the thyroids of $TR\beta^{PV/PV}$ mice than in wild types (Figure 5Aa, compare lanes 1–2 with 5–7). Consistent with the increased activation of the mTOR–p70S6K signalling and with the decreased FOXO3a nuclear activity (Figures 4g and h), we found that cyclin D1 levels were further increased by ~2-fold in $TR\beta^{PV/PV}Pten^{+/-}$ thyroids (Figure 5Aa, compare lanes 5–7 with 8–10). Dynactin-2 was used as the loading control (Figure 5Ab).

In addition to the AKT–FOXO3a pathway, we further examined the AKT–nuclear factor-κB (NF-κB) pathway to ascertain the effect of PTEN deficiency on the changes in apoptosis of thyroid tumour cells. The activation of AKT leads to an increased activity of NF-κB to block apoptosis and mediates tumour cell proliferation (Abdel-Latif *et al.*, 2008; Jiang and Liu, 2008). Figure 5B shows increased NF-κB protein levels in $TR\beta^{PV/PV}Pten^{+/-}$ thyroids (compare lanes 8–10 with 5–7, Figure 5Ba). Together with the increased phosphorylation of FOXO3a (Figures 4g and h), the increased NF-κB levels resulted in the inhibition of apoptosis that was evident by the decreased nuclear abundance of cleaved caspase-3 (compare Figures 5Ca and 5Cb with 5Cc and 5Cd). The reduced cleaved caspase-3 staining in the thyroid of $TR\beta^{PV/PV}Pten^{+/-}$ mice indicated decreased apoptotic activity mediated by decreased PTEN abundance. Altogether, these results indicate that PTEN deficiency led to further activation of cell proliferation and cell survival to promote thyroid tumour growth in $TR\beta^{PV/PV}$ mice.

Discussion

The inactivation and silencing of the *Pten* gene have been implicated in thyroid neoplasia (Di Cristofano *et al.*, 1998; Podsypanina *et al.*, 1999; Uppal *et al.*, 2007; Yeager *et al.*, 2007). However, despite many correlative data suggesting its deregulation could lead to thyroid cancer, direct *in vivo* evidence supporting this hypothesis was lacking. The availability of the $TR\beta^{PV/PV}$ mouse as a model of thyroid cancer presents us with an unusual opportunity to study directly the role of PTEN in thyroid carcinogenesis *in vivo*. This study shows that PTEN deficiency in $TR\beta^{PV/PV}$ mice dramatically accelerated and increased the occurrence of thyroid cancer progression and metastatic spread to the lung.

We recently found that the PI3K–AKT signalling pathways are activated in the thyroid tumours of $TR\beta^{PV/PV}$ mice (Furuya *et al.*, 2006), and that treatment of $TR\beta^{PV/PV}$ mice with the potent PI3K inhibitor, LY294002, effectively delays thyroid tumour progression and blocks metastatic spread (Furuya *et al.*, 2007). In the present study, we found that PTEN deficiency further increased the activation of AKT by an additional ~2 to 3-fold in the thyroids of $TR\beta^{PV/PV}$ mice. This additional AKT activation contributed to greater activation of the mTOR–p70S6K pathway to further increase tumour growth. We also found that PTEN deficiency further reduced the activity of the transcription factor FOXO3a in the thyroids of $TR\beta^{PV/PV}$ mice. FOXO3a positively regulates the transcription of proapoptotic genes and negatively regulates the transcription of cyclin D1 (Schmidt *et al.*, 2002). Consistent with these findings, PTEN deficiency resulted in ~2-fold increased cyclin D1 expression. Together with an activation of NF-κB, a decrease in apoptotic activity of thyroid cells was detected.

Altogether, our findings indicate that PTEN deficiency further activated AKT and altered AKT-downstream signalling pathways to increase cell proliferation and survival in $TR\beta^{PV/PV}$ thyroids, thereby accelerating thyroid cancer progression and invasiveness. We cannot exclude, however, that additional mechanisms involving PTEN-dependent but AKT-independent pathways (for review, see Blanco-Aparicio *et al.*, 2007) might have also exacerbated the thyroid cancer in $TR\beta^{PV/PV}Pten^{+/-}$ mice.

Because TSH is a major stimulator of thyrocyte growth, we compared serum TSH levels between $TR\beta^{PV/PV}$ mice with or without PTEN deficiency. In spite of marked accelerated thyroid tumour carcinogenesis in $TR\beta^{PV/PV}Pten^{+/-}$ mice (Figure 1), no significant differences in serum TSH levels were detected in $TR\beta^{PV/PV}$ mice with or without PTEN deficiency (Figure 2). These results suggested that the accelerated tumourigenesis of $TR\beta^{PV/PV}Pten^{+/-}$ thyroids mediated by PTEN deficiency did not involve the participation of TSH. The present findings are consistent with the observations in mice that selectively have lost the *Pten* gene in the thyroid ($Pten^{L/L}$*;TPO-Cre* mice; Yeager *et al.*, 2007). The selective loss of the *Pten* gene in the thyroid of $Pten^{L/L}$*;TPO-Cre* mice has no effect on the pituitary–thyroid axis, as these mutant mice have normal thyroid function tests (Yeager *et al.*, 2007). These mutant mice develop follicular adenoma, but no invasive tumours were observed up to 10 months of age. When TSH levels were elevated in these mutant mice, there was minimal effect on the proliferation and growth of thyrocytes of $Pten^{L/L}$*;TPO-Cre* mice. These findings indicate that TSH does not further increase thyrocyte proliferation mediated by the loss of the *Pten* gene. Thus, elevated TSH has no added synergistic effect on thyrocyte growth mediated by PTEN deficiency either in $TR\beta^{PV/PV}Pten^{+/-}$ mice or in $Pten^{L/L}$*;TPO-Cre* mice.

However, the findings that PTEN deficiency due to the loss of two alleles of the *Pten* gene resulted in follicular adenoma with no invasive tumours in $Pten^{L/L}$*;TPO-Cre* mice, but there was an accelerated tumour development in $TR\beta^{PV/PV}Pten^{+/-}$ mice (Figure 1) suggested that

the loss of the *Pten* gene alone is not sufficient to cause follicular thyroid carcinoma. This notion is consistent with the recent findings by Lu *et al.* (2007), in that thyroid cancer is excluded from the detected cancer spectrum in *R26-CreER;Pten* mice. We have shown earlier that PV physically interacts with the p85α subunit of PI3K and that this physical interaction increases the PI3K activity to activate the downstream AKT–mTOR–$p70^{s6k}$ signalling (Furuya *et al.*, 2006). This PV-mediated activation of the PI3K–AKT–mTOR–$p70^{s6k}$ signalling is blocked by the treatment of $TR\beta^{PV/PV}$ mice with LY294002, a potent and specific PI3K inhibitor, resulting in delaying thyroid tumour progression and prevention of metastatic spread (Furuya *et al.*, 2007). Reduced PTEN protein abundance in $TR\beta^{PV/PV}Pten^{+/-}$ mice further exacerbates tumour progression suggests that the deficiency in the PTEN-negative regulation leads to greater manifestation in the downstream signalling of PI3K activated by PV. Thus, the different phenotypes exhibited by $Pten^{L/L}$*;TPO-Cre* and $TR\beta^{PV/PV}Pten^{+/-}$ mice suggest that PV, by collaborating with multiple signalling pathways, functions as an oncogene to induce thyroid carcinogenesis in $TR\beta^{PV/PV}$ mice.

This study shows that PTEN deficiency led to accelerated thyroid cancer development, progression and invasion, thereby identifying *Pten* as an important tumour suppressor in thyroid carcinogenesis. Importantly, this mouse model offers an opportunity for the development of novel therapeutic targets in the PTEN–PI3K–AKT signalling pathway for the prevention and treatment of thyroid cancer.

Materials and methods

Mouse strains

The care and handling of the animals used in this study were approved by the National Cancer Institute Animal Care and Use Committee. Mice harbouring the *TRβPV* gene ($TR\beta^{PV/PV}$ mice) were prepared and genotyped as described earlier (Kaneshige *et al.*, 2000). $Pten^{+/-}$ mice were kindly provided by Dr Ramon Parsons (Columbia University, NY, USA; Podsypanina *et al.*, 1999). $TR\beta^{PV/PV}Pten^{+/-}$ mice were prepared by crossing $Pten^{+/-}$ mice with $TR\beta^{PV/+}$ mice, followed by crossing $TR\beta^{PV/+}Pten^{+/-}$ with $TR\beta^{PV/+}Pten^{+/+}$ mice. Littermates with a similar genetic background were used in all experiments. Mutant mice and wild-type littermates were euthanized to harvest thyroids for weighing, histological analysis and biochemical studies.

Western blot analysis

Preparation of whole cell lysates from thyroid glands has been described earlier (Kim *et al.*, 2005). Thyroids were homogenized on ice in lysis buffer containing 50 mM Tris, 100 mM HCl, 0.1% Triton X-100, 0.2 μM okadaic acid, 100 mM NaF and 2 mM Na_3VO_4 and a proteinase inhibitor tablet (Complete Mini EDTA-free; Roche, Mannheim, Germany), followed by incubation on ice for 10 min with occasional vortexing. The lysate was centrifuged for 5 min at 20 000 × *g* at 4 °C, and the supernatant was collected. The protein concentration for each lysate was determined by the Bradford assay (Pierce Chemical Co., Rockford, IL, USA) using BSA (Pierce Chemical Co.) as the standard. The protein sample (50 μg) was loaded and separated by SDS–polyacrylamide gel electrophoresis. After electrophoresis, the protein was electrotransferred to a polyvinylidene difluoride membrane (Immobilon-P; Millipore Corp., Bedford, MA, USA) as described by Furumoto *et al.* (2005). Antibodies were used according to the manufacturer's manuals at a 1:1000 dilution that included phosphorylated AKT (Ser473, no. 9271), AKT (no. 9272), phosphorylated mTOR (Ser2448, no. 2971), total mTOR (no. 2972), phosphorylated p70S6K (Thr421/Ser424, no. 9204), total p70S6K (no. 9202), PTEN (no. 9552), phosphorylated FOXO3a (no. 9466) and total FOXO3a (no. 9467) from Cell Signaling Technologies (Beverly, MA, USA). Cyclin D1 (SC-450, dilution 1:200) and anti-NF-κB antibodies (sc-372, 1:1000 dilution) were

purchased from Santa Cruz Biotechnology (Santa Cruz, CA, USA). Secondary antibodies used were horseradish peroxidase-conjugated goat anti-mouse or anti-rabbit IgG (Amersham Biosciences, Piscataway, NJ, USA). The loading controls were obtained from the same blot after being stripped with Re-Blot Plus (Chemicon, Temecula, CA, USA) and reprobed with rabbit polyclonal antibodies to dynactin-2 (AB5869P; Millipore, Billerica, MA, USA) or glyceraldehyde-3-phosphate dehydrogenase (no. 2118, 1:1000 dilution; Cell Signaling Technologies).

Histological analysis

Thyroid gland, lung, heart and lymph nodes were dissected and embedded in paraffin. Sections of 5 μm thickness were prepared and stained with haematoxylin and eosin. For each animal, single random sections through the thyroid, through the lung and through the heart were examined. For thyroids, morphological evidence of a single section of hyperplasia, capsular invasion, vascular invasion and anaplasia was routinely counted. Hyperplasia was generally diffused throughout the gland. Evidence of any of these changes in any section was counted as positive for that change. On average, in those cases with capsular invasion and/or vascular invasion, these morphological changes were seen in multiple locations (usually two or three) in any one single thyroid section. The presence of a single microscopic focus of metastatic follicular carcinoma in the lung was counted as positive for metastasis in that animal.

Immunohistochemistry

Histological sections were prepared as described earlier (Ying *et al.*, 2003). Detection of cleaved caspase-3 (no. 9661; Cell Signaling Technologies) by immunohistochemistry in paraffin sections was carried out as described earlier (Furuya *et al.*, 2007). Negative controls not including primary antibody were performed for each experiment.

Hormone assays

Total T4 and total T3 were determined by using a Clinical Assay GammaCoat T3 or T4 ^{125}I RIA Kit (DiaSolin, Stillwater, MN, USA), according to the manufacturer's instructions. Serum TSH levels were measured as described earlier (Furumoto *et al.*, 2005).

Statistical analysis

Statistical analysis was performed with the use of analysis of variance, and $P < 0.05$ was considered significant unless otherwise specified. StatView 5.0 was used to perform the Kaplan–Meier cumulative survival analysis, and Student's *t*-test using odds ratios and Fisher's exact probability test was used to analyse the data of pathological progression. GraphPad PRISM 4.0a (GraphPad Software, San Diego, CA, USA) was used for log-rank testing for statistical significance.

Acknowledgments

We thank Dr Hao Ying for assistance in the determination of thyroid function tests. This research was supported by the Intramural Research Program of Center for Cancer Research, National Cancer Institute, National Institutes of Health.

Abbreviations

AKT	protein kinase B
mTOR	mammalian target of rapamycin

PI3K	phosphatidylinositol 3-kinase
TRβ	thyroid hormone receptor β gene
TSH	thyroid-stimulating hormone

References

Abdel-Latif MM, Kelleher D, Reynolds JV. Potential role of NF-kappaB in esophageal adenocarcinoma: as an emerging molecular target. J Surg Res. 2008 (in press).

Blanco-Aparicio C, Renner O, Leal JF, Carnero A. PTEN, more than the AKT pathway. Carcinogenesis. 2007; 28:1379–1386. [PubMed: 17341655]

Di Cristofano A, Pesce B, Cordon-Cardo C, Pandolfi PP. Pten is essential for embryonic development and tumour suppression. Nat Genet. 1998; 19:348–355. [PubMed: 9697695]

Eng C. Role of PTEN, a lipid phosphatase upstream effector of protein kinase B, in epithelial thyroid carcinogenesis. Ann N Y Acad Sci. 2002; 968:213–221. [PubMed: 12119278]

Furumoto H, Ying H, Chandramouli GV, Zhao L, Walker RL, Meltzer PS, et al. An unliganded thyroid hormone beta receptor activates the cyclin D1/cyclin-dependent kinase/retinoblastoma/E2F pathway and induces pituitary tumorigenesis. Mol Cell Biol. 2005; 25:124–135. [PubMed: 15601836]

Furuya F, Hanover JA, Cheng SY. Activation of phosphatidylinositol 3-kinase signaling by a mutant thyroid hormone beta receptor. Proc Natl Acad Sci USA. 2006; 103:1780–1785. [PubMed: 16446424]

Furuya F, Lu C, Willingham MC, Cheng SY. Inhibition of phosphatidylinositol 3-kinase delays tumor progression and blocks metastatic spread in a mouse model of thyroid cancer. Carcinogenesis. 2007; 28:2451–2458. [PubMed: 17660507]

Greer EL, Brunet A. FOXO transcription factors at the interface between longevity and tumor suppression. Oncogene. 2005; 24:7410–7425. [PubMed: 16288288]

Guertin DA, Sabatini DM. Defining the role of mTOR in cancer. Cancer Cell. 2007; 12:9–22. [PubMed: 17613433]

Jiang BH, Liu LZ. PI3K/PTEN signaling in tumorigenesis and angiogenesis. Biochem Biophys Acta. 2008; 1784:150–158. [PubMed: 17964232]

Kaneshige M, Kaneshige K, Zhu X, Dace A, Garrett L, Carter TA, et al. Mice with a targeted mutation in the thyroid hormone beta receptor gene exhibit impaired growth and resistance to thyroid hormone. Proc Natl Acad Sci USA. 2000; 97:13209–13214. [PubMed: 11069286]

Kato Y, Ying H, Zhao L, Furuya F, Araki O, Willingham MC, et al. PPARgamma insufficiency promotes follicular thyroid carcinogenesis via activation of the nuclear factor-kappaB signaling pathway. Oncogene. 2006; 25:2736–2747. [PubMed: 16314832]

Kim CS, Vasko VV, Kato Y, Kruhlak M, Saji M, Cheng SY, et al. AKT activation promotes metastasis in a mouse model of follicular thyroid carcinoma. Endocrinology. 2005; 146:4456–4463. [PubMed: 16002527]

Li J, Yen C, Liaw D, Podsypanina K, Bose S, Wang SI, et al. PTEN, a putative protein tyrosine phosphatase gene mutated in human brain, breast, and prostate cancer. Science. 1997; 275:1943–1947. [PubMed: 9072974]

Liaw D, Marsh DJ, Li J, Dahia PL, Wang SI, Zheng Z, et al. Germline mutations of the PTEN gene in Cowden disease, an inherited breast and thyroid cancer syndrome. Nat Genet. 1997; 16:64–67. [PubMed: 9140396]

Lu TL, Chang JL, Liang CC, You LR, Chen CM. Tumor spectrum, tumor latency and tumor incidence of the Pten-deficient mice. PLoS ONE. 2007; 2:e1237, 1–13. [PubMed: 18043744]

Marsh DJ, Dahia PL, Zheng Z, Liaw D, Parsons R, Gorlin RJ, et al. Germline mutations in PTEN are present in Bannayan-Zonana syndrome. Nat Genet. 1997; 16:333–334. [PubMed: 9241266]

Meier CA, Dickstein BM, Ashizawa K, McClaskey JH, Muchmore P, Ransom SC, et al. Variable transcriptional activity and ligand binding of mutant beta 1 3,5,3′-triiodothyronine receptors from

four families with generalized resistance to thyroid hormone. Mol Endocrinol. 1992; 6:248–258. [PubMed: 1569968]

Nelen MR, van Staveren WC, Peeters EA, Hassel MB, Gorlin RJ, Hamm H, et al. Germline mutations in the PTEN/MMAC1 gene in patients with Cowden disease. Hum Mol Genet. 1997; 6:1383–1387. [PubMed: 9259288]

Neri LM, Borgatti P, Capitani S, Martelli AM. The nuclear phosphoinositide 3-kinase/AKT pathway: a new second messenger system. Biochim Biophys Acta. 2002; 1584:73–80. [PubMed: 12385889]

Parrilla R, Mixson AJ, McPherson JA, McClaskey JH, Weintraub BD. Characterization of seven novel mutations of the c-erbA beta gene in unrelated kindreds with generalized thyroid hormone resistance. Evidence for two 'hot spot' regions of the ligand binding domain. J Clin Invest. 1991; 88:2123–2130. [PubMed: 1661299]

Pervin S, Singh R, Chaudhuri G. Nitric oxide-induced cytostasis and cell cycle arrest of a human breast cancer cell line (MDA-MB-231): potential role of cyclin D1. Proc Natl Acad Sci USA. 2001; 98:3583–3588. [PubMed: 11248121]

Podsypanina K, Ellenson LH, Nemes A, Gu J, Tamura M, Yamada KM, et al. Mutation of Pten/Mmac1 in mice causes neoplasia in multiple organ systems. Proc Natl Acad Sci USA. 1999; 96:1563–1568. [PubMed: 9990064]

Ramaswamy S, Nakamura N, Sansal I, Bergeron L, Sellers WR. A novel mechanism of gene regulation and tumor suppression by the transcription factor FKHR. Cancer Cell. 2002; 2:81–91. [PubMed: 12150827]

Rivas M, Santisteban P. TSH-activated signaling pathways in thyroid tumorigenesis. Mol Cell Endocrinol. 2003; 213:31–45. [PubMed: 15062572]

Schlumberger M, Baudin E, Travagli JP. Papillary and follicular cancers of the thyroid. Presse Med. 1998; 27:1479–1481. [PubMed: 9798467]

Schmidt M, Fernandez de Mattos S, van der Horst A, Klompmaker R, Kops GJ, Lam EW, et al. Cell cycle inhibition by FoxO forkhead transcription factors involves downregulation of cyclin D. Mol Cell Biol. 2002; 22:7842–7852. [PubMed: 12391153]

Shepherd PR, Nave BT, Rincon J, Haigh RJ, Foulstone E, Proud C, et al. Involvement of phosphoinositide 3-kinase in insulin stimulation of MAP-kinase and phosphorylation of protein kinase-B in human skeletal muscle: implications for glucose metabolism. Diabetologia. 1997; 40:1172–1177. [PubMed: 9349598]

Sherman SI, Brierley JD, Sperling M, Ain KB, Bigos ST, Cooper DS, et al. Prospective multicenter study of thyroid carcinoma treatment: initial analysis of staging and outcome. National Thyroid Cancer Treatment Cooperative Study Registry Group. Cancer. 1998; 83:1012–1021. [PubMed: 9731906]

Steck PA, Pershouse MA, Jasser SA, Yung WK, Lin H, Ligon AH, et al. Identification of a candidate tumour suppressor gene, MMAC1, at chromosome 10q23.3 that is mutated in multiple advanced cancers. Nat Genet. 1997; 15:356–362. [PubMed: 9090379]

Suzuki A, de la Pompa JL, Stambolic V, Elia AJ, Sasaki T, del Barco Barrantes I, et al. High cancer susceptibility and embryonic lethality associated with mutation of the PTEN tumor suppressor gene in mice. Curr Biol. 1998; 8:1169–1178. [PubMed: 9799734]

Suzuki H, Willingham MC, Cheng SY. Mice with a mutation in the thyroid hormone receptor beta gene spontaneously develop thyroid carcinoma: a mouse model of thyroid carcinogenesis. Thyroid. 2002; 12:963–969. [PubMed: 12490073]

Uppal S, Mistry D, Coatesworth AP. Cowden disease: a review. Int J Clin Pract. 2007; 61:645–652. [PubMed: 17394437]

Wymann MP, Marone R. Phosphoinositide 3-kinase in disease: timing, location, and scaffolding. Curr Opin Cell Biol. 2005; 17:141–149. [PubMed: 15780590]

Yeager N, Klein-Szanto A, Kimura S, Di Cristofano A. Pten loss in the mouse thyroid causes goiter and follicular adenomas: insights into thyroid function and Cowden disease pathogenesis. Cancer Res. 2007; 67:959–966. [PubMed: 17283127]

Yen PM. Molecular basis of resistance to thyroid hormone. Trends Endocrinol Metab. 2003; 14:327–333. [PubMed: 12946875]

Ying H, Suzuki H, Furumoto H, Walker R, Meltzer P, Willingham MC, et al. Alterations in genomic profiles during tumor progression in a mouse model of follicular thyroid carcinoma. Carcinogenesis. 2003; 24:1467–1479. [PubMed: 12869418]

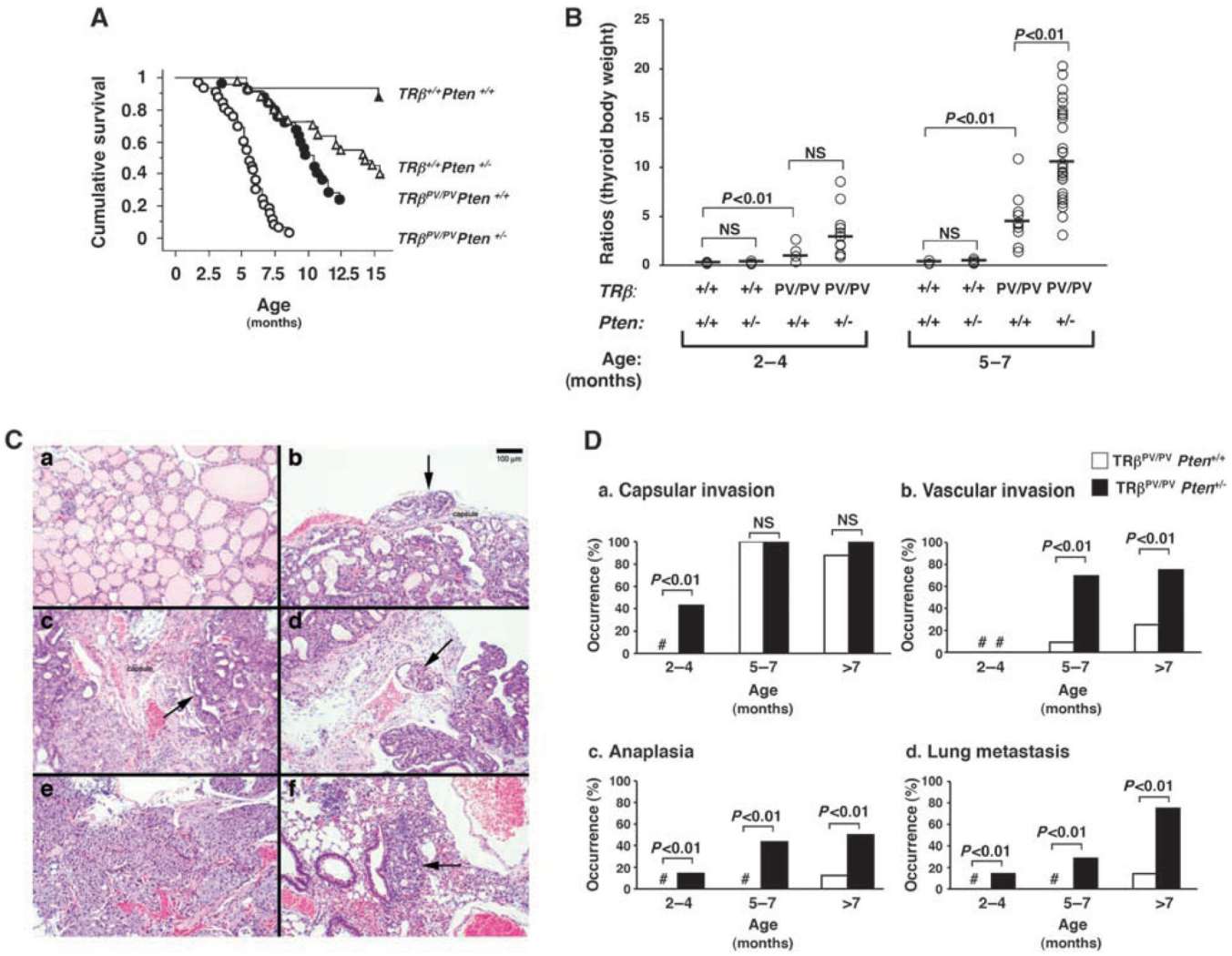

Figure 1.

(**A**) The Kaplan–Meier survival curves for *TR*β$^{+/+}$*Pten*$^{+/+}$, *TR*β$^{+/+}$*Pten*$^{+/−}$, *TRβ*$^{PV/PV}$*Pten*$^{+/+}$ and *TRβ*$^{PV/PV}$*Pten*$^{+/−}$ mice up to 15 months of age. The Kaplan–Meier cumulative survival analysis was performed using StatView 5.0. Survival rates of *TR*β$^{+/+}$*Pten*$^{+/−}$ (n = 33) and *TR*β$^{+/+}$*Pten*$^{+/+}$ wild-type (n = 16) mice are significantly different (P < 0.01); survival rates of *TRβ*$^{PV/PV}$*Pten*$^{+/+}$ (n = 25) and *TRβ*$^{PV/PV}$*Pten*$^{+/−}$ (n = 33) are significantly different (P < 0.01) and survival rates of *TR*β$^{+/+}$*Pten*$^{+/−}$ and *TRβ*$^{PV/PV}$*Pten*$^{+/−}$ are significantly different (P < 0.01). (**B**) Thyroid glands of *TR*β$^{+/+}$*Pten*$^{+/+}$ (n = 3–4), *TR*β$^{+/+}$*Pten*$^{+/−}$ (n = 4–10), *TRβ*$^{PV/PV}$*Pten*$^{+/+}$ (n = 4–10) and *TRβ*$^{PV/PV}$*Pten*$^{+/−}$ (n = 9–26) mice were dissected and compared in the same age groups. The data are presented as the ratios of thyroid weight to body weight. The difference in the thyroid weight between *TRβ*$^{PV/PV}$ mice with and without deletion of one *Pten* allele is significant at 5–7 months (P < 0.01), as determined by analysis of variance (ANOVA). (**C**) H&E staining of thyroids and lungs from (a) *TR*β$^{+/+}$*Pten*$^{+/−}$ (b) *TRβ*$^{PV/PV}$*Pten*$^{+/+}$ and (c–f) *TRβ*$^{PV/PV}$*Pten*$^{+/−}$ mice. (a) Normal thyroid of a *TR*β$^{+/+}$*Pten*$^{+/−}$ mouse aged 7 months. (b) Hyperplastic *TRβ*$^{PV/PV}$*Pten*$^{+/+}$ thyroid at 7 months of age showing an onset of capsular invasion (arrow). (c) Hyperplastic *TRβ*$^{PV/PV}$*Pten*$^{+/−}$ thyroid at 5 months of age displaying extensive capsular invasion (arrow), (d) vascular invasion (arrow) or (e) spindle cell anaplasia. (f) Lung metastases (arrow) in *TRβ*$^{PV/PV}$*Pten*$^{+/−}$ mouse. (**D**) Accelerated pathological progression of thyroid cancer in *TRβ*$^{PV/PV}$*Pten*$^{+/−}$ mice

as compared with $TR\beta^{PV/PV}Pten^{+/+}$ mice. Sections of thyroids and lungs from $TR\beta^{PV/PV}Pten^{+/+}$ ($n = 23$) and $TR\beta^{PV/PV}Pten^{+/-}$ ($n = 34$) mice were stained with H&E and analysed for age-dependent pathological progression of (a) capsular invasion, (b) vascular invasion, (c) anaplasia and (d) metastases in the lung. The data are expressed as the percentage of occurrence of total mutant mice examined. # indicates 0% occurrence.

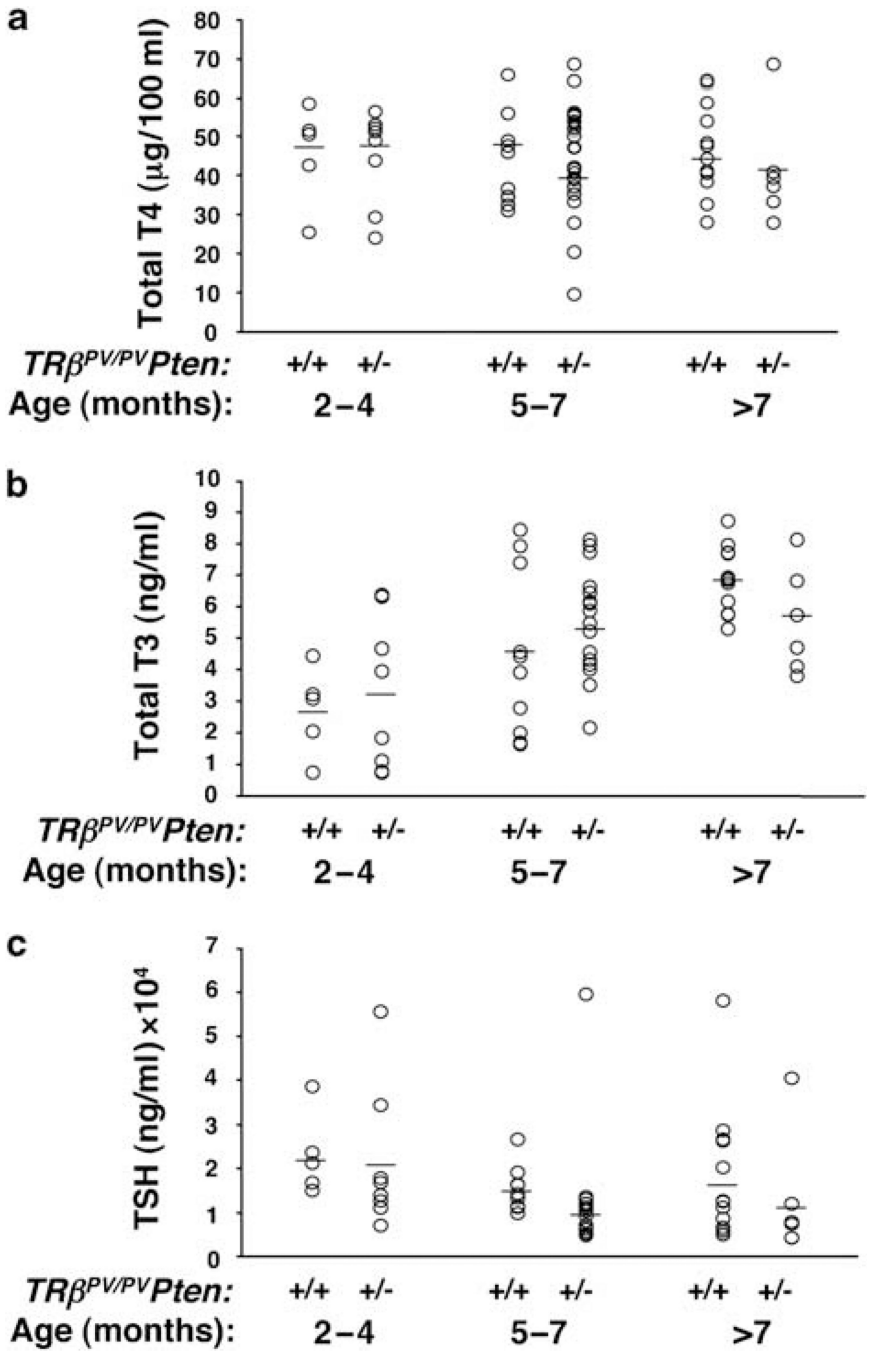

Figure 2.

No significant differences in thyroid function tests between $TR\beta^{PV/PV}Pten^{+/+}$ and $TR\beta^{PV/PV}Pten^{+/-}$ mice at different ages. Serum total T4 (**a**), total T3 (**b**) and TSH (**c**) of $TR\beta^{PV/PV}Pten^{+/+}$ (n = 9–12) mice, and $TR\beta^{PV/PV}Pten^{+/-}$ (n = 6–18) mice were determined at the ages indicated, as described in Materials and methods.

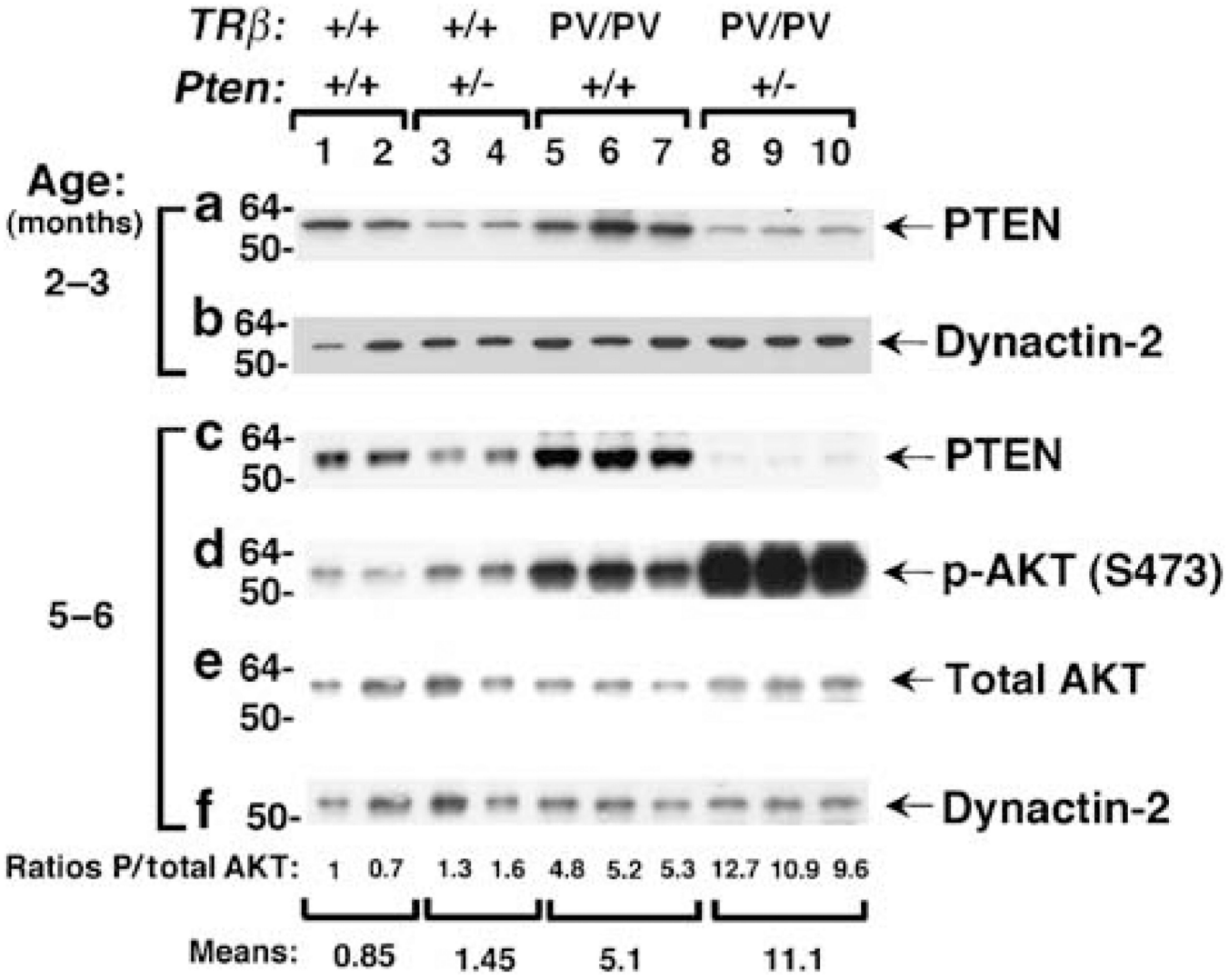

Figure 3.

Reduced abundance of PTEN protein and increased activation of AKT in $TR\beta^{PV/PV}Pten^{+/-}$ thyroids. Total protein extracts were prepared from thyroids of $TR\beta^{+/+}Pten^{+/+}$, $TR\beta^{+/+}Pten^{+/-}$ and thyroid tumours of $TR\beta^{PV/PV}Pten^{+/+}$ and $TR\beta^{PV/PV}Pten^{+/-}$ mice aged 2–3 months (**a** and **b**) and 5–6 months (**c**–**f**). Western blot analyses for PTEN (**a** and **c**), phosphorylated AKT (p-AKT) (**d**), total AKT (**e**) and dynactin-2 (**b** and **f**) as loading controls were carried out as described in Materials and methods. Representative results from two to three mice are shown and the genotypes are marked. The ratios of phosphorylated protein to total protein levels after quantification of the band intensities for each sample are indicated.

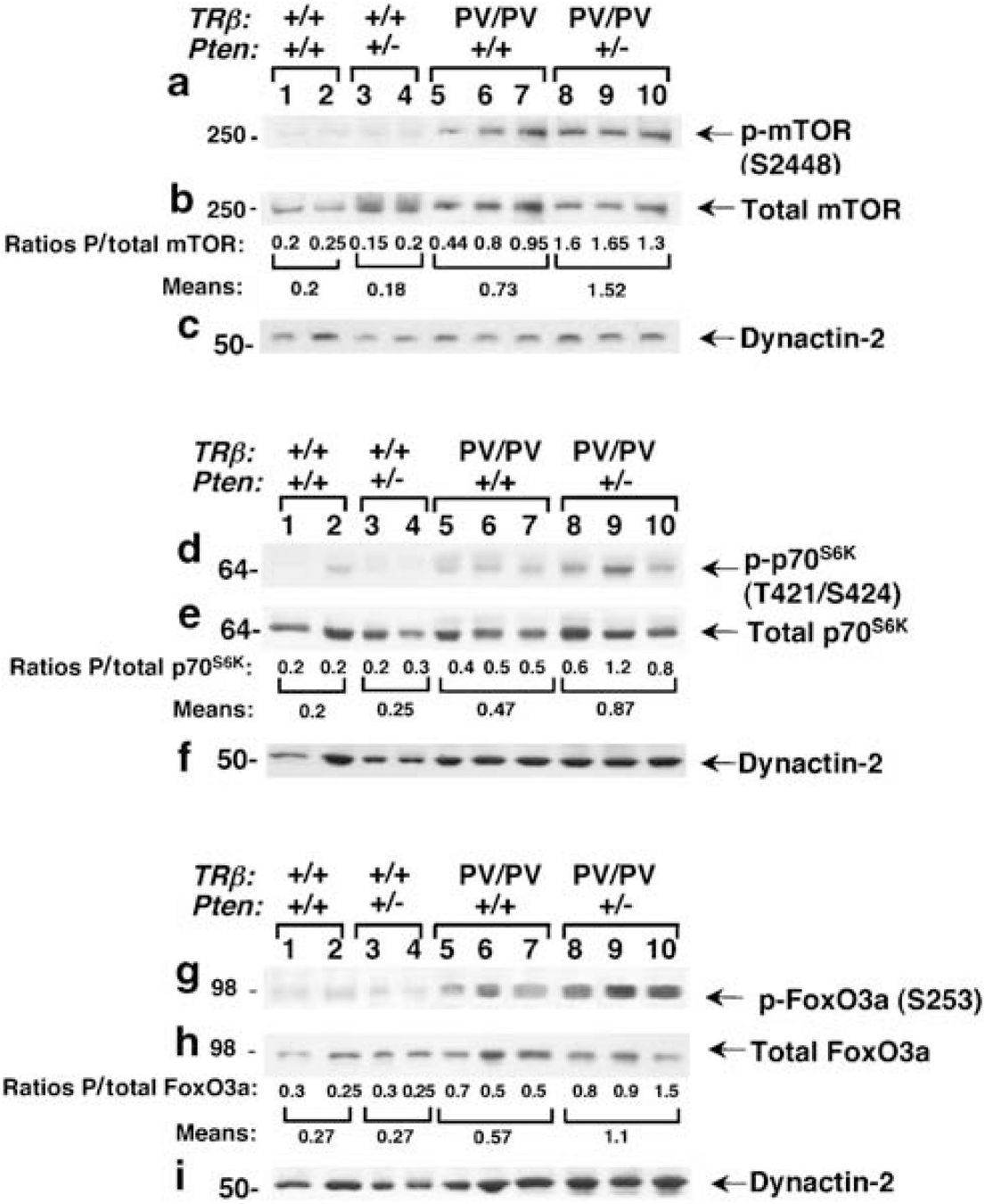

Figure 4.

Increased alteration in the AKT downstream signalling pathways in $TR\beta^{PV/PV}$ mice induced by PTEN deficiency. Total protein extracts were prepared from thyroids of $TR\beta^{+/+}Pten^{+/+}$ and $TR\beta^{+/+}Pten^{+/-}$ and from thyroid tumours of $TR\beta^{PV/PV}Pten^{+/+}$ and $TR\beta^{PV/PV}Pten^{+/-}$ mice, aged 5–6 months. Western blot analysis was carried out for (**a**) phosphorylated mTOR (p-mTOR), (**b**) total mTOR, (**c**) Dynactin-2, (**d**) phosphorylated p70S6K (p-p70S6K), (**e**) total p70S6K, (**f**) Dynactin-2, (**g**) phosphorylated FOXO3a (p-FOXO3a), (**h**) total FOXO3a and (**i**) Dynactin-2, as described in Materials and methods. The littermates with different genotypes were used in the analysis. Representative results from two to three mice are

shown and the genotypes marked. The ratios of phosphorylated protein to total protein levels after quantification of the band intensities for each sample are indicated.

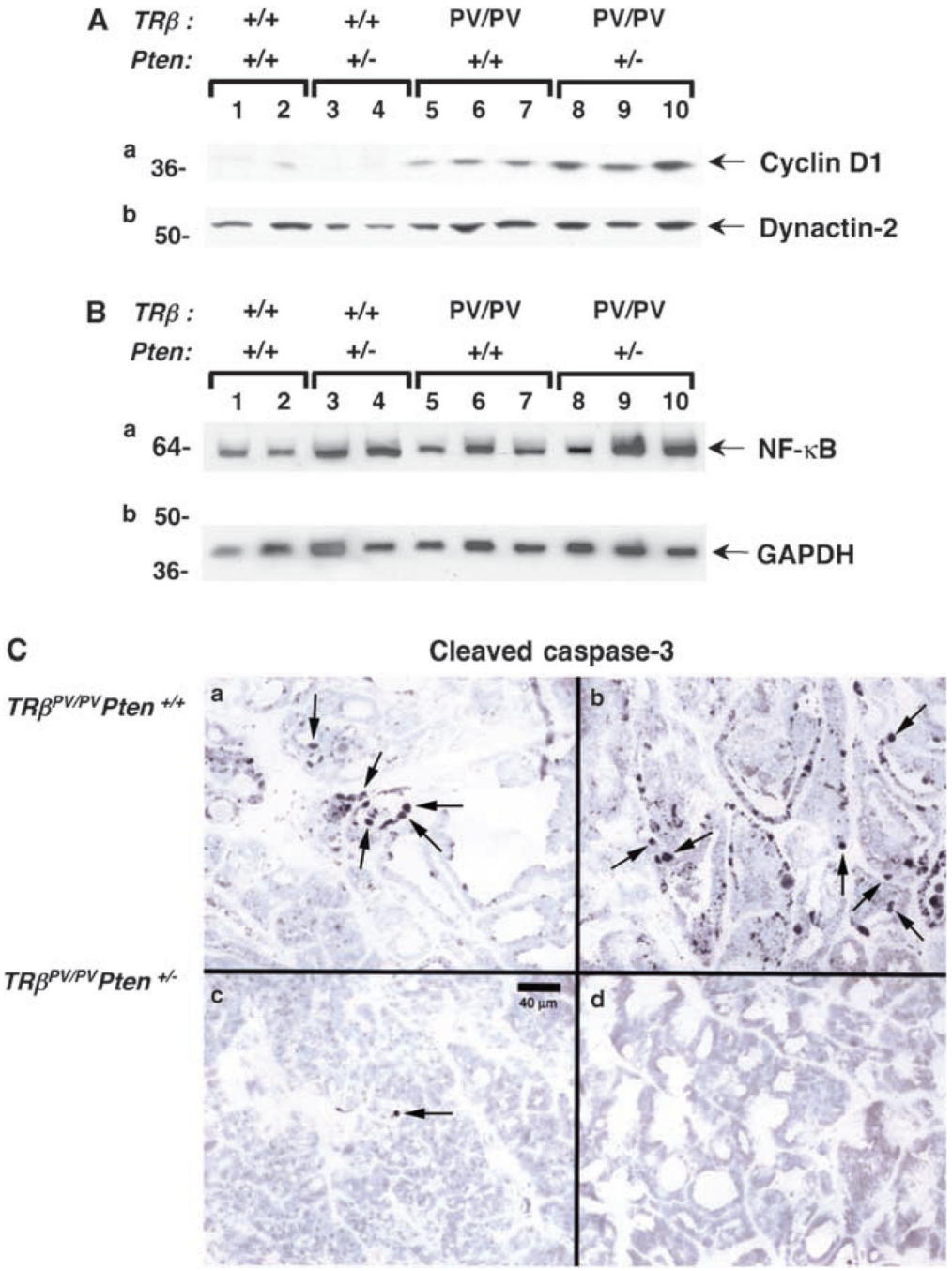

Figure 5.

Increased cell-cycle progression and cell survival in $TR\beta^{PV/PV}$ mice with PTEN deficiency. Total protein extracts were prepared from thyroids of $TR\beta^{+/+}Pten^{+/+}$ and $TR\beta^{+/+}Pten^{+/-}$, and from thyroid tumours of $TR\beta^{PV/PV}Pten^{+/+}$ and $TR\beta^{PV/PV}Pten^{+/-}$ mice. Western blot analysis was carried out for (**A**a) Cyclin D1, (**A**b) Dynactin-2, (**B**a) NF-κB and (**B**b) GAPDH. The littermates with different genotypes were used in the analysis. (**C**) Reduced apoptotic activity of thyroid tumour cells of $TR\beta^{PV/PV}Pten^{+/-}$ (c and d) mice as compared with $TR\beta^{PV/PV}Pten^{+/+}$ (a and b). Immunostaining of cleaved caspase-3 was carried as described in Materials and methods. In the thyroid of $TR\beta^{PV/PV}Pten^{+/-}$ mice, very few

thyroid cells show cleaved caspase-3 labelling (arrow) as compared with $TR\beta^{PV/PV}Pten^{+/+}$ thyroids.

Table 1

Thyroid tumour progression in $TR\beta^{PV/PV}Pten^{+/+}$, $TR\beta^{PV/PV}Pten^{+/-}$ and $TR\beta^{+/+}Pten^{+/-}$ female and male mice

Genotype	Sex	No.	50% survival rate age (months)	Thyroid tumour (%)				
				Hyperplasia	Capsular invasion	Vascular invasion	Anaplasia	Lung metastasis
$TR\beta^{PV/PV}Pten^{+/+}$	Female	11	11.6	100	78	22[a]	0	11.1[a]
	Male	14	9.4	100	75	8.3	8.3[a]	0
$TR\beta^{PV/PV}Pten^{+/-}$	Female	19	5.8	100	52	34.7	34.7	30.4[a]
	Male	14	5.2	100	60	33	33	20
$TR\beta^{+/+}Pten^{+/-}$[b,c]	Female	13	12.2[a]	0	0	0	0	0
	Male	20	15	0	0	0	0	0

[a] A significant difference ($P < 0.05$) between females and males of the same genotype.

[b] Histological characteristics obtained from $TR\beta^{+/+}Pten^{+/-}$ mice aged 4.7–16.5 months.

[c] Multiple abnormalities were found in $TR\beta^{+/+}Pten^{+/-}$ mice, including lymphoma, splenomegaly and endometrium neoplasia, as described earlier (Podsypanina *et al.*, 1999).